Ultrafast and steady-state laser heating effects on electron relaxation and phonon coupling mechanisms in thin gold films

Patrick E. Hopkins, John C. Duda, Bryan Kaehr, Xiao Wang Zhou, C.-Y. Peter Yang, and Reese E. Jones

Citation: Applied Physics Letters **103**, 211910 (2013); doi: 10.1063/1.4833415
View online: http://dx.doi.org/10.1063/1.4833415
View Table of Contents: http://scitation.aip.org/content/aip/journal/apl/103/21?ver=pdfcov
Published by the AIP Publishing

Ultrafast and steady-state laser heating effects on electron relaxation and phonon coupling mechanisms in thin gold films

Patrick E. Hopkins,[1,a)] John C. Duda,[1] Bryan Kaehr,[2,3] Xiao Wang Zhou,[4] C.-Y. Peter Yang,[4] and Reese E. Jones[4]
[1]*Department of Mechanical and Aerospace Engineering, University of Virginia, Charlottesville, Virginia 22904, USA*
[2]*Advanced Materials Laboratory, Sandia National Laboratories, Albuquerque, New Mexico 87106, USA*
[3]*Department of Chemical and Nuclear Engineering, University of New Mexico, Albuquerque, New Mexico 87106, USA*
[4]*Sandia National Laboratories, Livermore, California 94550, USA*

(Received 30 July 2013; accepted 10 November 2013; published online 22 November 2013)

We study the scattering mechanisms driving electron-phonon relaxation in thin gold films via pump-probe time-domain thermoreflectance. Electron-electron scattering can enhance the effective rate of electron-phonon relaxation when the electrons are out of equilibrium with the phonons. In order to correctly and consistently infer electron-phonon coupling factors in films on different substrates, we must account for the increase in steady-state lattice temperature due to laser heating. Our data provide evidence that a thermalized electron population will not directly exchange energy with the substrate during electron-phonon relaxation, whereas this pathway can exist between a non-equilibrium distribution of electrons and a non-metallic substrate. © *2013 AIP Publishing LLC*. [http://dx.doi.org/10.1063/1.4833415]

A thorough understanding of the relaxation mechanisms of hot electrons in solids is critical to an array of applications. For example, laser processing of solids with sub-picosecond laser pulses relies on rapid absorption of the pulse energy by electrons, traversal of these hot electrons away from the surface, and subsequent electron-phonon interactions that lead to melting, ablation, and spallation.[1–6] The rate of electronic relaxation during and after pulse absorption dictates the electron and phonon temperatures. As a result, electron-phonon coupling is a critical pathway of energy conversion due to the non-equilibrium induced by short pulse laser heating.

Despite this, the fundamental scattering mechanisms driving hot electron relaxation with a surrounding lattice are still very much up for debate. In Kaganov's original derivation,[7] the electron-phonon coupling factor, G, was hypothesized to be constant at temperatures much greater than the Debye temperature, i.e., $T \gg \Theta_D$. This hypothesis was later derived using superconducting theory[8] and confirmed experimentally.[9] However, these confirming measurements were conducted in a regime of negligible electron-phonon non-equilibrium (i.e., $T_e - T_p \ll T_p$, where T_e and T_p are the electron and phonon temperatures, respectively). When $T_e - T_p$ is large, additional electronic scattering mechanisms beyond the electron-phonon interaction can affect the rate at which the electron system loses energy; these mechanisms include electron scattering at grain boundaries,[10] defects,[11] material interfaces,[12–14] and d-band holes.[5,6,15] Generally speaking, many of these mechanisms are relatively unstudied due the lack of experimental evidence demonstrating the interplay between T_e and T_p and their subsequent influence on electron-phonon relaxation.

In response, we perform a series of measurements designed to investigate the influence of electron temperature, interfacial structure, and lattice temperature on electron relaxation dynamics in Au films after short pulse laser heating. By measuring the effective electron-phonon coupling factor, G_{eff}, in Au films on rough Si substrates, we find that interfacial roughness only affects electron-phonon relaxation at high T_e.[13,16] In addition, we measure G_{eff} in Au films on glass substrates and find that G_{eff} is independent of substrate so long as changes in T_p that arise from steady-state laser heating are accounted for. Furthermore, we present a consistent set of analyses to interpret pump-probe reflectivity data, correlate these data to thermal responses of the electron and phonon systems, and describe interactions between them with a two temperature model (TTM).[17] Using this procedure, we are able to show that transient reflectivity data in the low perturbation limit can be used to calculate the electron-electron and electron-phonon collisional frequencies (ν_{ee} and ν_{ep}, respectively). We use these results to evaluate the current understanding of electron relaxation and the influence of T_e and T_p, thereby providing a more comprehensive picture of electron dynamics in thin films during and after short pulse laser heating.

Our experiments are carried out using the time-domain thermoreflectance (TDTR) technique, which is described in detail elsewhere.[18–20] Several aspects of our apparatus deserve explicit attention in the context of the present work: (i) the pump path is frequency doubled from 1.55 to 3.1 eV; (ii) the pump and probe pulses at the sample surface are approximately 400 and 200 fs, respectively (pump pulses are stretched due to extra optics along the pump path, e.g., the electro-optic modulator); (iii) pump and probe $1/e^2$ radii are $6.1 \pm 0.7\,\mu$m and $5.2 \pm 0.6\,\mu$m, respectively; and (iv) the average probe power incident on the sample surface is 9 mW

a)Electronic mail: phopkins@virginia.edu

while the pump power is varied between 9 and 116 mW. Absorption of the pump pulses by the electrons in the Au films yields electron temperatures that are initially higher than the phonon temperature. This temperature difference creates a situation in which electron-phonon relaxation is the primary mechanism driving electronic cooling. We monitor the change in reflectivity of the sample with the probe beam at the frequency with which we modulate the pump beam (11.39 MHz). The measured signal can be correlated to electron temperature with an appropriate reflectivity model.

We evaporate 20 nm Au films on Si and glass substrates and several of the Si substrates are roughened prior to Au deposition (details of sample preparation and characterization are given in Ref. 21). Film thicknesses are confirmed via picosecond acoustics.[22,23] We calculate the absorbed power in the Au films with thin-film-on-substrate optics calculations[24,25] and confirm these calculations with near normal ($<5^\circ$) reflectivity measurements of the pump and probe beams. Our measurements and calculations agree to within 5%.

Example TDTR data taken on a 20 nm Au film on a Si substrate using two different incident pump laser powers (corresponding to the listed calculated absorbed laser fluences) are plotted in Fig. 1. We use the procedure that we have outlined previously to determine the rate of electron relaxation.[26] Since our probe beam energy is well below the interband transition threshold of Au (Ref. 1) and our maximum electron temperatures do not excite d-band electrons,[15] we use a Drude-based thermoreflectivity model in our analysis.[27,28] We do not expect a substantial change in conduction band number density due to interband transitions induced by the pump pulse.[29,30]

In order to properly convert the measured change in reflectivity to the change in temperature, we must have

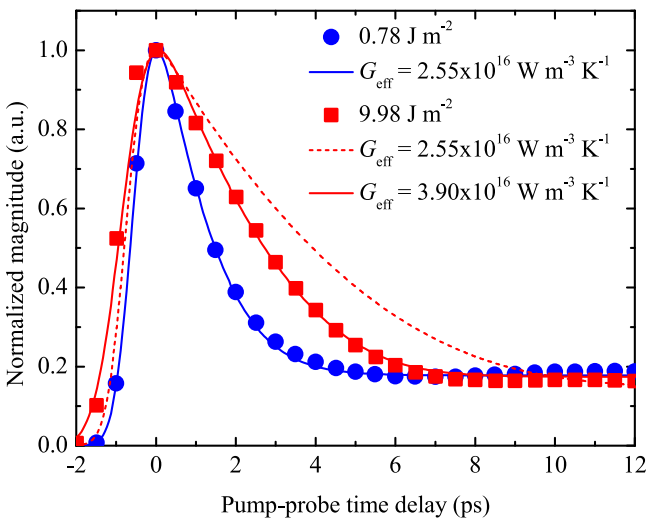

FIG. 1. TDTR data on 20 nm Au/Si samples at two different fluences (circles and squares) and corresponding fits using the thermoreflectance model and TTM described in the text. At low fluences (blue circles and line) and correspondingly low electron temperatures, the best fit model results in G_{eff} that is in good agreement with the previous measurements (Refs. 9 and 26). At high fluences (red squares and line) which results in larger temperature differences between the electrons and phonons, the best fit model results in an increase in G_{eff}. Assuming the TTM parameters are constant with temperature, the model agreement with the data is poor at high fluences (dashed line).

accurate knowledge of the electron-electron and electron-phonon collisional frequencies. For metals, these frequencies are dependent on temperature: $\nu_{ee} = A_{ee}T_e^2$ and $\nu_{ep} = B_{ep}T_p$. Typically, the scattering coefficients A_{ee} and B_{ep} are estimated from low temperature electrical resistivity data.[31] This is valid for temperatures at which the electron density of states is relatively constant in energy space; for Au, this corresponds to $T_e \leq 3,500$ K.[15] However, this is assumption is not valid for metals with highly varying densities of states around the Fermi energy. To ensure the generality of our work, we establish a procedure to directly measure the scattering coefficients from TDTR data that can be applied to any metallic system. This is described below with our procedure for measuring G_{eff} in our samples.

Electron relaxation in our thin films is described by our modified variation of the TTM to account for a film with thickness less than the ballistic electron relaxation length and a delayed electron thermalization time.[17,26] Thermal coupling between the electron and phonon systems in the Au films is governed by G_{eff}; G_{eff} is distinct from the intrinsic rate of electron-phonon coupling in a metal, G, since G should not be affected by electron-electron or electron-interface scattering.[15] However, the measured response in a film is a convolution of all of these relaxation mechanisms.

Before fitting the TTM to our TDTR data to determine G_{eff}, we must relate the measured change in reflectivity to the change in electron temperature due to the laser pulse. To do so, we require knowledge of thermoreflectance model parameters A_{ee} and B_{ep}. We replace G_{eff} in the TTM with[32]

$$G_{\text{eff}} = \frac{\pi^2 m_e v_s^2 n_e}{6}\left(A_{ee}(T_e + T_p) + B_{ep}\right), \tag{1}$$

where m_e is the free electron mass, v_s is the Debye speed of sound, and n_e is the free electron number density. With A_{ee} and B_{ep} as free parameters, we fit the TTM to low-fluence TDTR data and find $A_{ee} = 1.5 \times 10^7\ \text{K}^{-2}\ \text{s}^{-1}$ and $B_{ep} = 1.3 \times 10^{11}\ \text{K}^{-1}\ \text{s}^{-1}$, which are in excellent agreement with literature values.[2,33] We caution that this approach may not necessarily be valid when electron scattering mechanisms with different temperature dependencies are prominent. As we expect these coefficients to be constant in Au for $T_e \leq 3,500$ K (the onset of d-band transitions and a change in free electron density in gold), we use these best-fit scattering coefficients as constants throughout the remainder of our analysis. This approach should be valid to determine ν_{ee} and ν_{ep} for any metal given relatively small perturbations of the electron temperature (i.e., $T_e - T_p \leq T_p$), offering a robust method to measure electron scattering frequencies.

Using our values of A_{ee} and B_{ep}, we fit the TTM to our TDTR data by normalizing the peak electron temperature to the peak in our data and adjusting G_{eff}. We fit the data before the peak by accounting for a delay in thermalization of the electron system.[26] In agreement with the previous data on electron thermalization time in Au,[26,34–38] we find thermalization time of the excited electrons in our experiments is between 800 fs to 1.1 ps. This implies that the electron system is nearly fully thermalized during electron-phonon relaxation, as discussed by Guo *et al.*[14] We find that for all fluences and samples, only minor adjustments to A_{ee} and B_{ep}

(by less than 10%) are necessary to achieve a best fit. This yields acceptable agreement of our model to the data over the entire time span of our measurements from before pulse absorption to several ps after electron-phonon equilibration. This approach is more robust and offers less uncertainty compared to other approaches for determining G_{eff} since only normalization at the time of maximum signal is required to achieve model and data agreement. These TTM fits to our TDTR data are plotted solid lines in Fig. 1. The best fit G_{eff} increases with increasing laser fluence (discussed in more detail later).

Figure 2 shows the best fit values of G_{eff} as a function of absorbed fluence for the Au/Si samples. For TTM fits, we assume experimentally observed values for the free electron heat capacity from Ref. 39, lattice heat capacities of Au tabulated from Ref. 40, and we take the thermal penetration depth of the electrons as the film thickness (20 nm), consistent with the previous observations and analyses accounting for an increased ballistic electron relaxation length in Au.[1,26] As is clear from Fig. 2, the effective rate of relaxation of the excited electron system increases as the absorbed fluence increases. However, we note that the magnitude of the increase that we observe in this work is much smaller than our previous observations,[13,16] which we discuss in detail below.

We examine contribution of interfacial imperfections to this increase in G_{eff} by repeating measurements using Si substrates of varying roughness. The fabrication procedure of these rough samples is described in our previous work.[21] We note that the Au films demonstrated intimate contact to the substrate,[21] and therefore the only difference between the various rough samples is the substrate surface roughness. However, it should be noted that we allowed a native oxide to reform on the silicon surface prior to Au evaporation (confirmed via microscopy), and therefore the Au is only weakly mechanically coupled to the silicon substrates. We find that

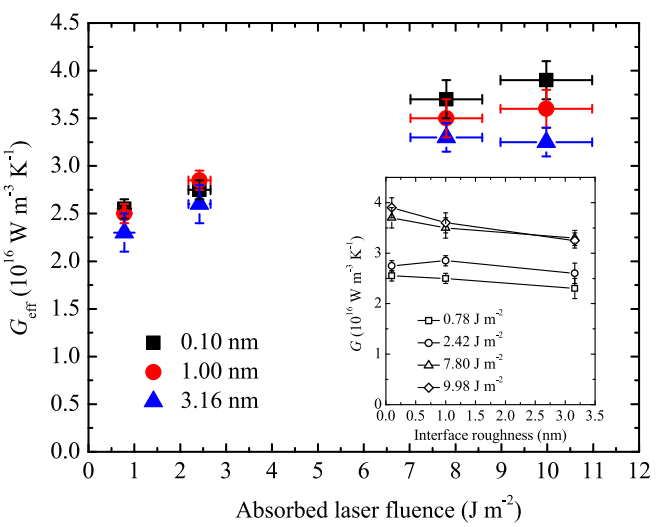

FIG. 2. G_{eff} as a function of absorbed laser fluence and interface roughness. At increased fluences resulting in an increase in peak electron temperature, the electron system relaxes with the phonons more readily, indicating an increase in inelastic electron scattering events leading to energy loss from the electron system. An increase in RMS roughness leads to a decrease in G_{eff} as the peak electron temperature increases; this is clear in the inset which shows G_{eff} as a function of Si RMS roughness.

G_{eff} is non-negligibly affected by substrate roughness only at increased laser fluence. To show this more clearly, we plot G_{eff} as a function of Si RMS roughness (as measured via atomic force microscopy) in the inset of Fig. 2. The decrease of G_{eff} with roughness only becomes pronounced at higher absorbed fluences. This implies that this electron-relaxation mechanism (i.e., electron-interface scattering) is impeded by interfacial roughness. From this, we infer that increased electron-interface scattering decreases G_{eff} in a fully thermalized electron system; note, this is different from our previous observations in data on thin film Au using a different laser system[13,16] which we discuss in detail later.

To examine the influence of T_p on electronic relaxation during laser heating, we measure G_{eff} in 20 nm Au films on glass substrates. The average laser power absorbed by the Au film leads to a local temperature rise in the film and substrate (heat sink). We refer to this as the steady state, or DC, heating, which is inversely proportional to the thermal conductivity of the heat sink.[41,42] Using an approximation for steady state temperature rise,[42] the absorbed laser power, and the thermal conductivity of the glass substrate (1.12 W m^{-1} K^{-1} as measured via additional TDTR thermal effusivity measurements), we estimate that the Au lattice temperature rise in our measurements on the Au/glass samples ranges from $\Delta T_{DC} = 138 - 423$ K above room temperature, $T_0 = 298$ K. We illustrate the necessity of accounting for this steady state heating in Fig. 3(a), where the best-fit values of G_{eff} on our Au/glass samples are plotted as a function of maximum electron temperature. Not accounting for an increased initial temperature in the TTM leads to a best-fit

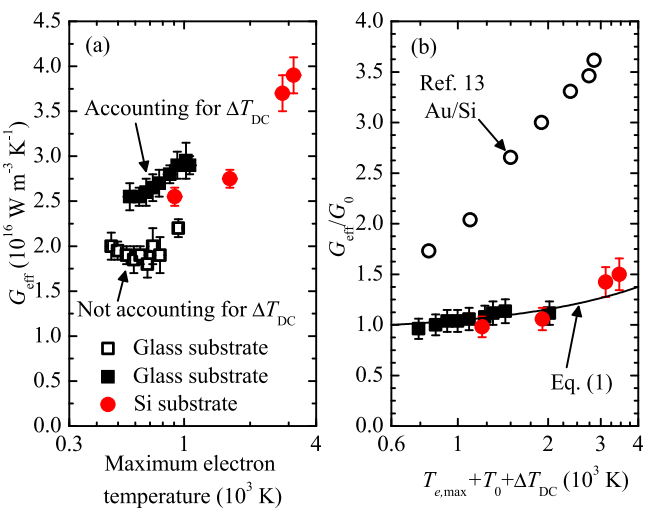

FIG. 3. (a) G_{eff} as a function of maximum electron temperature for the Au/glass samples and the "smoothest" Au/Si sample. Not accounting for the steady state lattice temperature rise in the glass samples leads to a measured G_{eff} that is not consistent with the Au/Si data. However, accounting for ΔT_{DC} in TTM fits to the Au/glass data results in similar electron temperature trends between the determined G_{eff} for Au/glass and Au/Si interfaces. (b) G_{eff} as a function of maximum electron temperature plus steady state lattice temperature. The results in (a) imply that the mechanisms driving G_{eff} are intrinsic to the Au and are independent of the glass or Si substrate. This is confirmed through the agreement of our data to Eq. (1). However, we observed a much larger enhancement in G_{eff} in our previous work in which electron relaxation was occurring when the electrons were not in a thermal distribution (Ref. 13). Therefore, we postulate that electrons in a non-Fermi distribution lose energy more readily to the substrate than electrons in a Fermi distribution.

value of G_{eff} that is nearly constant with electron temperature and also lower than the previously measured, accepted value of G in Au in the low perturbation regime ($G_0 = 2.6 \times 10^{16}$ W m^{-3} K^{-1}, Ref. 26). However, accounting for ΔT_{DC} when fitting for G_{eff} leads to values for G_{eff} in the low perturbation regime that agree well with the accepted value for G_0 in addition to showing similar trends with electron temperature as our Au/Si measurements. We note that as electron temperature increases, it becomes more important to account for DC heating from the average laser power. Therefore, in higher fluence pulsed laser applications, steady state laser heating must be accounted for in electron-phonon thermal processes.

To understand the competing scattering mechanisms driving our observed values of G_{eff}, we replot the data from Fig. 3(a) in Fig. 3(b) as a function of $T_e + T_p$ and normalize both the data and the model by G_0 (Refs. 9 and 26), thus allowing for a direct comparison of the data to the model. We find excellent agreement between our current data and Eq. (1), indicating that the increase in G_{eff} that we observe in our data is driven by an increase in electron-electron scattering rates in the Au films (in Eq. (1), the electron-electron scattering term is the only term directly affected by T_e and T_p). Therefore, electron-electron scattering plays an increased role in the overall rate of electron relaxation with the lattice as the energy density in the electron system increases. This can also be used to explain our observed trends with substrate roughness in Fig. 2; since our Au films are less than the ballistic electron relaxation length, disorder in the Au caused by the interface roughness leads to a reduction in G_{eff}. Therefore, the roughness affects the electron-electron scattering rate, which as we mention above, is the underlying mechanism driving the temperature dependency in G_{eff}. This is consistent with the previous theories showing that vibrating boundaries and impurities in a metallic film will decrease the overall rate of electron relaxation with the lattice.[43] This also presents a unique method to explicitly measure the role of impurities on electron-phonon equilibration in thin metal films by inducing disorder on the surface of a substrate then depositing metals with thickness less than the ballistic electron relaxation length for TDTR measurements.

Finally, we address the issue of a thermalized vs. non-thermalized electron distribution interacting at the metal/non-metal interface. In Fig. 3(b), we show the results from our previous study of the measured G_{eff} in 20 nm Au/Si samples using a 150 fs laser pulse.[16] In these data, the rise time of the TDTR data (before zero pump-probe delay time) was $\approx$200 fs, as compared to the rise time in our current data: $\approx$800 fs to 1.1 ps (see Fig. 1). Due to the well known delay in thermalization in Au, there was most probably a significant portion of the electron system that was in a non-thermal state during the temporal regime of electronic relaxation (i.e., after zero pump-probe delay time).[34–37] In this case, we observed a large increase in G_{eff} that cannot be explained by increased electron-electron scattering (i.e., Eq. (1)). We attributed this to ballistic electron interface scattering and subsequent thermal boundary conductance (interfacial thermal transport). However, in our present study, G_{eff} is measured in a regime where the majority of the electrons are in a thermal, Fermi distribution due to the long rise time of data,[26] and our data are well described by Eq. (1) without needing to account for interface scattering. Therefore, we postulate that the enhancement in thermal boundary conductance and hot electron relaxation beyond that predicted via Eq. (1) is driven by ballistic electrons in a non-thermal, nonequilibrium distribution. In other words, we theorize that electrons in a non-Fermi distribution will interact more readily with an interface and lose more energy to the substrate compared to electrons in a Fermi distribution.

Recent work from Guo *et al.*[14] observed this increase in G_{eff} and also attributed this to a hot-electron, interface-scattering-driven thermal boundary conductance. The authors report this phenomena in a regime in which the electrons are in a thermal distribution. In work of Guo *et al.*, however, the laser fluences applied to their gold films were over an order of magnitude higher than the fluences applied in our present study. Therefore, we cannot directly compare our current data to their results due to changes in the electron number density and d-band excitations which can affect electron-phonon scattering, heat capacity, and absorption.[14,29,33,44] Regardless, there have been previous observations of enhancement in G_{eff} due to interfacial transport channels associated with ballistic electrons, and the origin and scattering mechanisms driving this enhancement are only beginning to become clear.

In summary, we have studied the electron scattering mechanisms driving electron-phonon equilibration in 20 nm Au films on silicon and glass substrates. We find that for a thermalized (i.e., Fermi) electron distribution, electron-electron scattering can enhance the overall rate of electron-phonon relaxation at high electron temperatures. In addition, we find that increased Au/substrate interface scattering induced from surface roughness decreases the rate electron-phonon relaxation. This is in contrast to recent works showing that interfaces can enhance electron-phonon relaxation. However, we attribute this difference to the state of the electron system: if the majority of the electrons are described by a non-equilibrium distribution, electrons can lose energy to the substrate. However, if the electrons are thermalized, we show no evidence that electron thermal energy will be lost to the substrate. The exact mechanisms driving the elastic vs. inelastic electron-interface interaction are unclear, and future works should investigate the interplay between electron thermalization, ballistic transport, and thermal relaxation in thin films both theoretically and experimentally. Potential studies include examining the electron relaxation mechanisms in metals with different grain sizes, defect concentrations and thicknesses on substrates that are either conducting or insulating.

P.E.H. recognizes support from the AFOSR Young Investigator Program (No. FA9550-13-1-0067). This work was performed under a Laboratory Directed Research and Development (LDRD) project through Sandia National Laboratories. Sandia National Laboratories is a multi-program laboratory managed and operated by Sandia Corporation, a wholly owned subsidiary of Lockheed Martin Corporation, for the U.S. Department of Energy's National Nuclear Security Administration under Contract No. DE-AC04-94AL85000.

[1]J. Hohlfeld, S. S. Wellershoff, J. Gudde, U. Conrad, V. Jahnke, and E. Matthias, Chem. Phys. **251**, 237 (2000).
[2]D. S. Ivanov and L. V. Zhigilei, Phys. Rev. B **68**, 064114 (2003).
[3]I. H. Chowdhury and X. Xu, Numer. Heat Transfer, Part A **44**, 219 (2003).
[4]L. V. Zhigilei, D. S. Ivanov, E. Leveugle, B. Sadigh, and E. M. Bringa, Proc. SPIE **5448**, 505 (2004).
[5]W. L. Chan, R. S. Averback, D. G. Cahill, and A. Lagoutchev, Phys. Rev. B **78**, 214107 (2008).
[6]W. L. Chan, R. S. Averback, D. G. Cahill, and Y. Ashkenazy, Phys. Rev. Lett. **102**, 095701 (2009).
[7]M. I. Kaganov, I. M. Lifshitz, and L. V. Tanatarov, Sov. Phys. JETP **4**, 173 (1957).
[8]P. B. Allen, Phys. Rev. Lett. **59**, 1460 (1987).
[9]W. Wang and D. G. Cahill, Phys. Rev. Lett. **109**, 175503 (2012).
[10]T. Q. Qiu and C. L. Tien, J. Heat Transfer **115**, 842 (1993).
[11]A. Sergeev and V. Mitin, Phys. Rev. B **61**, 6041 (2000).
[12]A. V. Sergeev, Phys. Rev. B **58**, R10199 (1998).
[13]P. E. Hopkins, J. L. Kassebaum, and P. M. Norris, J. Appl. Phys. **105**, 023710 (2009).
[14]L. Guo, S. L. Hodson, T. S. Fisher, and X. Xu, J. Heat Transfer **134**, 042402 (2012).
[15]Z. Lin, L. V. Zhigilei, and V. Celli, Phys. Rev. B **77**, 075133 (2008).
[16]P. E. Hopkins and P. M. Norris, Appl. Surf. Sci. **253**, 6289 (2007).
[17]S. I. Anisimov, B. L. Kapeliovich, and T. L. Perel'man, Sov. Phys. JETP **39**, 375 (1974).
[18]A. J. Schmidt, X. Chen, and G. Chen, Rev. Sci. Instrum. **79**, 114902 (2008).
[19]P. E. Hopkins, J. R. Serrano, L. M. Phinney, S. P. Kearney, T. W. Grasser, and C. T. Harris, J. Heat Transfer **132**, 081302 (2010).
[20]D. G. Cahill, K. E. Goodson, and A. Majumdar, J. Heat Transfer **124**, 223 (2002).
[21]J. C. Duda, C.-Y. P. Yang, B. M. Foley, R. Cheaito, D. L. Medlin, R. E. Jones, and P. E. Hopkins, Appl. Phys. Lett. **102**, 081902 (2013).
[22]C. Thomsen, J. Strait, Z. Vardeny, H. J. Maris, J. Tauc, and J. J. Hauser, Phys. Rev. Lett. **53**, 989 (1984).
[23]C. Thomsen, H. T. Grahn, H. J. Maris, and J. Tauc, Phys. Rev. B **34**, 4129 (1986).
[24]F. Abeles, in *Advanced Optical Techniques*, edited by A. C. S. V. Heel (North-Holland Publishing Co., Amsterdam, 1967), pp. 145–188.
[25]P. E. Hopkins, Phys. Rev. B **81**, 035413 (2010).
[26]P. E. Hopkins, L. M. Phinney, and J. R. Serrano, J. Heat Transfer **133**, 044505 (2011).
[27]A. N. Smith and P. M. Norris, Appl. Phys. Lett. **78**, 1240 (2001).
[28]P. E. Hopkins, J. Appl. Phys. **105**, 093517 (2009).
[29]P. E. Hopkins, Appl. Phys. Lett. **96**, 041901 (2010).
[30]It is important to note that the pump pulses, which will excite interband transitions in Au given its 3.1 eV photon energy, will modify the number of electrons in the 6*s* shell of Au due to optical excitations from the 5*d* shell. This can affect the thermoreflectance modeling if the number of excited electrons from the 5*d* shell becomes a substantial portion of the conduction band number density in the 6*s* shell, especially during sub-picosecond time regimes where electrons are thermalizing and ballistically traversing through the Au with a non-Fermi distribution.[29] However, calculations from our previous work[29] confirm that even at our maximum absorbed laser fluence (9.98 J m^{-2}), the conduction band number density will only be perturbed by $<2\%$, which we conclude will negligibly affect our proper determination of transient electron temperature using the Drude-based thermoreflectance model.[29]
[31]M. Kaveh and N. Wiser, Adv. Phys. **33**, 257 (1984).
[32]J. K. Chen, W. P. Latham, and J. E. Beraun, J. Laser Appl. **17**, 63 (2005).
[33]X. Y. Wang, D. M. Riffe, Y.-S. Lee, and M. C. Downer, Phys. Rev. B **50**, 8016 (1994).
[34]C. K. Sun, F. Vallee, L. H. Acioli, E. P. Ippen, and J. G. Fujimoto, Phys. Rev. B **48**, 12365 (1993).
[35]C. K. Sun, F. Vallee, L. H. Acioli, E. P. Ippen, and J. G. Fujimoto, Phys. Rev. B **50**, 15337 (1994).
[36]W. S. Fann, R. Storz, H. W. K. Tom, and J. Bokor, Phys. Rev. Lett. **68**, 2834 (1992).
[37]W. S. Fann, R. Storz, H. W. K. Tom, and J. Bokor, Phys. Rev. B **46**, 13592 (1992).
[38]R. H. M. Groeneveld, R. Sprik, and A. Lagendijk, Phys. Rev. B **51**, 11433 (1995).
[39]C. Kittel, *Introduction to Solid State Physics*, 7th ed. (John Wiley and Sons, Inc., New York, 1996).
[40]F. Incropera and D. P. DeWitt, *Fundamentals of Heat and Mass Transfer*, 4th ed. (Wiley and Sons, Inc., New York, 1996).
[41]D. G. Cahill, Rev. Sci. Instrum. **75**, 5119 (2004).
[42]A. Schmidt, M. Chiesa, X. Chen, and G. Chen, Rev. Sci. Instrum. **79**, 064902 (2008).
[43]A. Sergeev, B. S. Karasik, M. Gershenson, and V. Mitin, Physica B **316–317**, 328 (2002).
[44]P. E. Hopkins and D. A. Stewart, J. Appl. Phys. **106**, 053512 (2009).